

# Amide Proton Transfer Imaging for Differentiation of Glioblastoma from Brain Metastasis

Utarat Kaewumporn MD<sup>1</sup>, Doonyaporn Wongsawaeng MD<sup>1</sup>, Siriwan Piyapittayanan MD<sup>1</sup>, Chanon Ngamsombat MD<sup>1</sup>, Panid Chaysiri MD<sup>2</sup>, Janiya Kittikornchaichan BSc<sup>2</sup>, Kritidipha Ningunha MD<sup>3</sup>, Nanthasak Tisavipat MD<sup>3</sup>, Titima Itthimathin MD<sup>3</sup>, Ketkanok Rayaruji BSc<sup>3</sup>, Orasa Chawalparit MD<sup>1</sup>

<sup>1</sup> Division of Diagnostic Radiology, Department of Radiology, Faculty of Medicine Siriraj Hospital, Mahidol University, Bangkok, Thailand

<sup>2</sup> Division of Radiotherapy, Department of Radiology, Faculty of Medicine Siriraj Hospital, Mahidol University, Bangkok, Thailand

<sup>3</sup> Bangkok International Hospital, BDMS, Bangkok, Thailand

**Objective:** To evaluate the difference in amide proton transfer (APT)-weighted imaging between glioblastoma and brain metastasis.

**Materials and Methods:** Fourteen patients including eight males and six females, with age ranging between 46 and 75 years old, were included in the present study. Ten patients with glioblastomas and four patients with brain metastases underwent preoperative brain 3T-MRI with APT-weighted sequence. The magnetization transfer ratio asymmetry (MTRasym) and normalized magnetization transfer ratio asymmetry (nMTRasym) values in enhancing solid portion, peritumoral non-enhancing hyperintense FLAIR area, and contralateral normal appearing white matter (CNAWM) in glioblastomas and brain metastases were obtained and compared for statistical analyses. Final diagnosis was validated by pathological results.

**Results:** The MTRasym and nMTRasym in enhancing solid portion and peritumoral non-enhancing hyperintense FLAIR area of glioblastomas were significantly greater than that of the brain metastases. By visual assessment, the APTw color map also showed higher signal at the perilesional edema in glioblastomas than the metastasis.

**Conclusion:** As a non-invasive imaging method, APT-weighted MR imaging might be helpful to distinguish glioblastomas from brain metastasis.

**Keywords:** Amide proton transfer weighted imaging; Glioblastomas; Brain metastasis

Received 22 November 2021 | Revised 2 November 2022 | Accepted 22 November 2022

**J Med Assoc Thai 2022;105(12):1224-9**

**Website:** <http://www.jmatonline.com>

Amide proton transfer weighted (APTw) imaging, a novel molecular non-gadolinium magnetic resonance imaging (MRI) technique based on chemical exchange-saturation transfer (CEST) principle, has been designed to detect amide protons in low-concentration endogenous mobile proteins and peptides in the tissue<sup>(1)</sup> by means of protons exchange with nearby bulk water. The APTw signal is related to cell density and endogenous mobile proteins and peptides<sup>(2)</sup>.

APTw imaging has emerged as a valuable tool for grading brain tumors<sup>(3)</sup>, distinguishing tumor recurrence from radiation necrosis<sup>(4)</sup>, pseudo-progression from true progression in gliomas<sup>(5)</sup>, primary central nervous system lymphomas from gliomas<sup>(6)</sup>, and benign meningioma from atypical meningioma<sup>(7,8)</sup>.

Glioblastomas (GBM) and brain metastasis are commonly encountered in adult population. The ability to distinguish them is crucial because of difference in therapeutic process. Up to now, advanced MRI techniques, such as diffusion, perfusion, and magnetic resonance (MR) spectroscopy have been used to differentiate these two tumors<sup>(9-12)</sup> but still have limitations and inconclusive findings.

Few previous studies had focused on differentiating between GBM and brain metastasis by using APTw imaging<sup>(9,13)</sup>. Yu et al<sup>(9)</sup> found higher APTw value of peritumoral area of GBM than single brain metastasis (SBM) but no difference between these two tumor cores. Kamimura et al<sup>(13)</sup> concluded that APT signal in peritumoral area may not be an efficient tool for distinguishing GBM and SBM. These

## Correspondence to:

Wongsawaeng D.

Division of Diagnostic Radiology, Department of Radiology, Faculty of Medicine Siriraj Hospital, Mahidol University, 2 Wanglang Road, Bangkok 10700, Thailand.

**Phone:** +66-2-4197086, **Fax:** +66-2-4127785

**Email:** [Doonyaporn.wos@mahidol.edu](mailto:Doonyaporn.wos@mahidol.edu)

## How to cite this article:

Kaewumporn U, Wongsawaeng D, Piyapittayanan S, Ngamsombat C, Chaysiri P, Kittikornchaichan J, et al. Amide Proton Transfer Imaging for Differentiation of Glioblastoma from Brain Metastasis. *J Med Assoc Thai* 2022;105:1224-9.

**DOI:** 10.35755/jmedassocthai.2022.12.13715

results required further investigation.

The authors hypothesized that the APTw values of tumor mass and peritumoral area may provide quantitative information on tumor cellularity and perilesional microenvironment and might be useful to differentiate GBM from brain metastasis.

## Materials and Methods

### Study populations

The present study was approved by the Institutional Ethics Committees (No. SI824/2020, and No. BHQ 2020-45). The present study was a retrospective multi-center study from two tertiary hospitals. Nineteen MRI studies from 14 patients with eight males and six females and a median age of 64.5 years old with a range of 46 to 75 years old, were recruited between July 2019 and December 2019. They were diagnosed as GBM in 10 cases and metastatic brain in four cases.

### MRI data

MRI was performed with a 3.0-T MRI scanner (Ingenia, Philips Medical System, Best, the Netherlands) with a 32-channel head coil. The conventional imaging protocol including T1W, T2W, T2W/FLAIR, and postcontrast T1W images was performed.

APT image was acquired before gadolinium administration by using the 3D spin-echo approach. The imaging parameters were as follows: repetition time (TR)/echo time (TE) 6491/7.8 ms; voxel size 1.8×1.8 mm, matrix 256×256, slice thickness 6.0 mm, turbo spin-echo factor 174, and echo planar imaging factor 1. The z-axis coverage was 10 slices. For saturation, a pulse-train radiofrequency saturation with saturation power at 2 μT and saturation time for 2.0 seconds was used. Multi-offset was done with offsets at 0, ±0.25, ±0.5, ±0.75, ±1, ±1.5, ±2, ±2.5, ±3, ±3.25, ±3.5, ±3.75, ±4, ±4.5, ±5, and ±6 ppm. The total acquisition time was four minutes. The APT color map was generated from software at the MRI workstation and sent to PACS system together with all conventional MRI images.

### Image analysis

The qualitative and quantitative image analyses were consensus-based performed together by the two observers, which are a 10-year-experience (DW) and a 5-year-experience (UK) neuroradiologists on the commercially available software (Philips IntelliSpace Portal). The regions of interest (ROIs) were performed in round shaped and placed into various regions

including Gd-enhancing tumor area, peritumoral non-enhancing T2W/FLAIR hyperintense area, and contralateral normal-appearing white matter (CNAWM). The ROIs on APTw source image were identified by using Gd-T1W or T2W/FLAIR images. Each ROI was placed in one best representative place in each single enhancing area and its adjacent peritumoral T2W/FLAIR hyperintense area. Careful attempts were made to exclude cystic or necrotic portions. Note that some necrotic portions were attempted placing ROIs without quantitative analysis inclusion. The size of each ROI was 6.46 mm<sup>2</sup>. All the APTw values from each ROIs were displayed in mean ± standard deviation (SD) [referring to the calculated magnetization transfer ratio asymmetry (MTR<sub>asym</sub>) range from -5% to +5%]<sup>(14)</sup>. Finally, normalized MTR<sub>asym</sub> (nMTR<sub>asym</sub>) values were calculated as follows: nMTR<sub>asym</sub> = MTR<sub>asym</sub>(tumor) – MTR<sub>asym</sub>(NAWM), where MTR<sub>asym</sub>(tumor) was the mean MTR<sub>asym</sub> of ROIs in enhancing or non-enhancing tumors, and MTR<sub>asym</sub>(NAWM) was the mean MTR<sub>asym</sub> of ROIs in corresponding CNAWM<sup>(7,15)</sup>.

### Statistical analysis

Descriptive statistics were presented as numbers, percentages, mean, SD, median, and minimum-maximum as appropriate. All parametric and non-parametric data were tested for normal distribution before further appropriate statistical analysis.

The comparison of the qualitative data used chi-square or the Fisher's exact test. The comparison of the quantitative data used independent-samples t-test or Mann-Whitney U test. The p-value less than 0.05 indicated a statistically significant difference. The statistical analysis was performed using PASW Statistics, version 18.0 (SPSS Inc., Chicago, IL, USA).

## Results

### Qualitative visual assessment

**Glioblastoma** (Figure 1): On APT color map, all gadolinium-enhancing solid portion had corresponding high signal on APTw image demonstrated as yellow color. Almost perilesional non-enhancing hyperintense FLAIR areas also showed high APT signal seen as yellow color. However, a few perilesional hyperintense FLAIR regions showed no increased APT signal demonstrated as green color as background normal white matter.

**Metastatic brain tumor** (Figure 2): All 11 metastatic lesions had the same color shading on

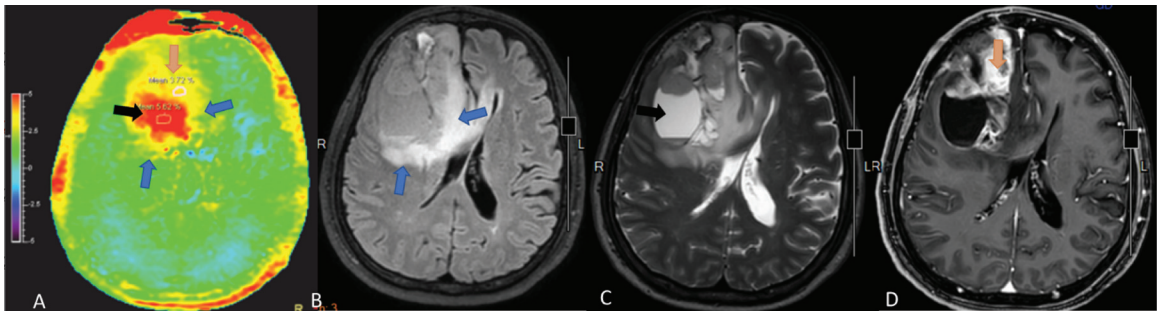


**Figure 1.** APT-weighted and conventional MR images of a 62-year-old male with glioblastoma at right frontal lobe. APT color map (A) showed yellow color corresponding with the enhancing solid portion in Gd-enhanced T1W-image (D) (orange arrow). Necrotic portion (black arrow) showed red color on APT color map (A) with turbid fluid SI on FLAIR image (B) and high SI on T2W image (C). Two peritumoral hyperintense FLAIR regions showed yellow color on APT color map (A) (blue arrow) comparing to background green color of normal white matter.

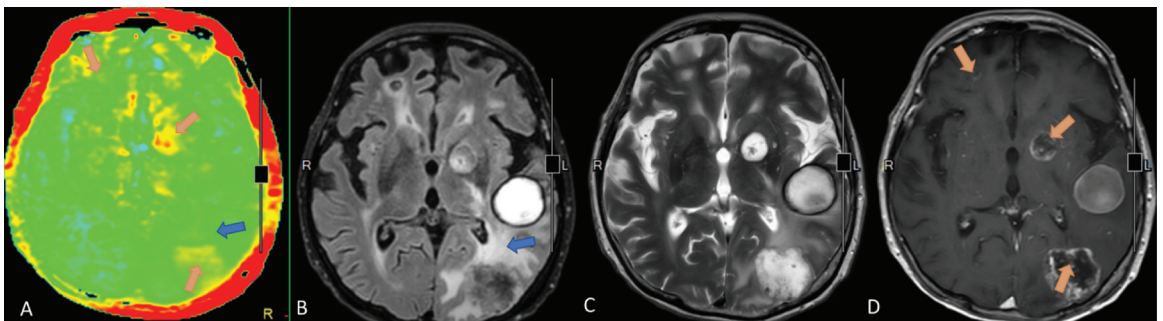


**Figure 2.** APT-weighted and conventional MR images of a 68-year-old female with multiple metastatic breast cancer lesions (2 irregular rim-enhancing lesions at left temporo-occipital lobe and left basal ganglia and 1 tiny faint enhancing lesion at right frontal lobe). APT color map (A) showed yellow color corresponding with enhancing component with high conspicuity on left basal ganglia and left temporo-occipital lesions (D) (orange arrow). The perilesional hyperintense on FLAIR (B) and T2W (C) at left temporo-occipital region show green color on APT color map (A) (blue arrow) which indistinguishable from the normal brain background. Note that the hyperintense T1W lesion at left temporal lobe was not performed ROI (pre-Gd T1W not shown).

APT color map as GBM group for enhancing solid portion but not for perilesional non-enhancing hyperintense FLAIR areas, which showed green color inseparable from the normal background.

### Quantitative assessment

Nineteen MRI studies from 14 patients were pathologically diagnosed, including 10 GBM and four brain metastases. The four patients with metastases were from three breast carcinoma and one carcinoma of unknown origin.

The quantitative evaluation was performed in every lesion in these studies. Patients with more than one lesions were quantified in every lesion. Patients with more than one studies were evaluated separately as individual lesion. There were 19 lesions of GBM group as two patients with three follow-up images, one patient with two follow-up images, and three patients with multicentric/multifocal GBM, and 11 lesions of metastasis group. All metastatic

and multicentric/multifocal GBM lesions were pathologically diagnosed only one lesion for each patient.

The median age with minimum-maximum, gender, MTR<sub>asym</sub>, and nMTR<sub>asym</sub> (showed as mean±SD) between the GBM and metastasis groups are shown in Table 1. The MTR<sub>asym</sub> and nMTR<sub>asym</sub> values of the enhancing solid portion of GBM were significantly higher than that of brain metastases as  $2.90 \pm 1.01$  versus  $1.83 \pm 0.95$  for MTR<sub>asym</sub> and  $2.24 \pm 1.14$  versus  $1.36 \pm 0.90$  for nMTR<sub>asym</sub> ( $p < 0.05$ ).

The peritumoral non-enhancing hyperintense FLAIR area also showed the same phenomenon with the enhancing part which significantly higher APT values than that of brain metastases as  $1.92 \pm 1.04$  versus  $1.11 \pm 0.45$  for MTR<sub>asym</sub>, and  $1.44 \pm 1.17$  versus  $0.65 \pm 0.53$  for nMTR<sub>asym</sub>, respectively ( $p < 0.05$ ).

### Discussion

Advanced MRI techniques are used increasingly

**Table 1.** Demographic data and APT results of glioblastomas and metastatic brain tumor

	GBM	Metastasis	p-value
Clinical characteristics			
Number of patients	10	4	
Age (years); median (min, max)	66.0 (51.0, 75.0)	56.5 (46.0, 74.0)	0.285
Sex (% of male/female)	70/30	25/75	0.245
APT parameters			
Number of lesions	19	11	
MTRAsym; mean±SD			
• Enhancing solid portion	2.90±1.01	1.83±0.95	0.008
• Peritumoral high FLAIR area	1.92±1.04	1.11±0.45	0.021
nMTRAsym; mean±SD			
• Enhancing solid portion	2.24±1.14	1.36±0.90	0.037
• Peritumoral high FLAIR area	1.44±1.17	0.65±0.53	0.043

GBM=glioblastomas; APT=amide proton transfer; MTRAsym=magnetization transfer ratio asymmetry; nMTRAsym=normalized magnetization transfer ratio asymmetry; SD=standard deviation; FLAIR=fluid-attenuated inversion recovery

to obtain physiologic and metabolic information that complements the anatomic information provided by conventional MRI<sup>(16)</sup>. Advanced MRI techniques such as diffusion, perfusion MRI, and MR spectroscopy to differentiate between these tumors are still controversial<sup>(11,12,14,16)</sup>.

APT imaging is one of non-contrast enhancement technique by indirect detection of metabolites with exchangeable protons<sup>(17)</sup> using selective irradiation at 3.5 ppm downfield of the water resonance to saturate amide protons in the tissue<sup>(18)</sup>. The APT signal can be quantified using the saturation percentage of the water signal to detect concentration of endogenous mobile proteins and peptides in biological tissue<sup>(16)</sup>.

In the present study, the APTw images were generated using the optimal saturation power of 2 μT, which achieved approximately zero APTw intensity, as green, in normal brain tissue, allowing easy identification of hyperintensities, as yellow to red. The premise underlying its potential utility is that certain diseases such as malignant tumors with high cellularity may exhibit elevated APT values<sup>(19)</sup>.

The MTRAsym values or APTw values of the tumor and normal brain tissue are affected by various tissue microenvironment and technical factors. Therefore, the authors evaluated the diagnostic value of APT imaging based on nMTRAsym, the difference in MTRAsym between tumors and normal brain tissue, because it is minimally affected by non-physiologic factors<sup>(7)</sup>.

The present study showed the mean MTRAsym values and the mean nMTRAsym values at enhancing solid portions of GBM to be significantly higher than

those in brain metastases ( $p<0.05$ ) same as Kamimura et al<sup>(13)</sup> but differed from Yu et al study<sup>(9)</sup>.

Although the mechanism for the higher APTw value in GBM compared to brain metastases is unclear, Kamimura et al<sup>(13)</sup> suggests the contribution from protein-rich extracellular matrix filling the extracellular spaces may explain the high APTw value<sup>(20)</sup>.

In addition, previous studies reported that the high-grade gliomas had higher concentration of mobile proteins and peptides than the low-grade gliomas<sup>(2,16,21)</sup>. Park et al<sup>(21)</sup> considered that APT MRI is a promising in vivo imaging method for quantifying the cellular proliferation of gliomas. These findings imply that the higher APTw signal intensity in the higher-grade gliomas attributed to the denser cellularity in the solid components of these tumors.

Chiang et al<sup>(12)</sup> reported the mean ADC values at contrast enhancing areas of metastases to be significantly higher than those in high-grade gliomas. The higher ADC in metastases suggests higher intracellular and extracellular water fractions than in high-grade glioma. However, ADC values could delineate areas of neoplastic cell infiltration. This implies that GBM may usually have higher neoplastic cell infiltration than metastases.

The mean MTRAsym value (APTw value) of GBM in the present study showed value of 2.90±1.01, which was concordant to cut off median values of 2.23 and range of 1.53 to 3.7, from the previous meta-analysis study<sup>(22)</sup>.

The mean MTRAsym values and the mean nMTRAsym values at peritumoral non-enhancing hyperintense FLAIR area of GBM were significantly higher than those in brain metastases ( $p<0.05$ ) in the present study, which is the same as Yu et al<sup>(9)</sup> but different from Kamimura et al<sup>(13)</sup>.

Previous advanced MRI studies including diffusion, perfusion, and MR spectroscopy have shown that peritumoral hyperintense FLAIR area of metastases brain tumors reflect vasogenic edema. In the GBM, it was hypothesized that specific cells and inflammatory cells infiltrated into the perilesional zone, and that the perilesional zone of FLAIR hyperintensity reflects more than just vasogenic edema<sup>(12,16)</sup>.

The discrepant results between the study and previous ones<sup>(9,13)</sup>, either in enhancing portion or peritumoral hyperintense FLAIR area of GBM and brain metastasis, may be explained by differences in APTw MRI acquisition and metastatic in origin. Kamimura et al used a 2D single axial slice of the

maximum cross-sectional area of tumor while the present study employed 3D with 10 axial slices with more tumor coverage for analysis. Metastatic in origin predominance may also cause population bias lung cancer for Kamimura et al study<sup>(13)</sup> and breast cancer for the present study. However, the pathophysiology behind area suspected of peritumoral vasogenic edema is still unknown. Histological data remains essential tool.

For visual assessment, the present study found that APTw signal of perilesional non-enhancing hyperintense FLAIR areas in glioblastoma usually showed high signal, as seen in 15 of 19 lesions, demonstrated as yellow color, whereas all metastatic perilesional non-enhancing hyperintense FLAIR areas showed green color inseparable from normal white matter background on APT color map. On the contrary, all enhanced portions of both glioblastoma and brain metastases showed increased APT signal as demonstrated by the same yellow shade on APT color map. Therefore, visual assessment on APT color map might be capable to differentiate these two tumors.

For reported gadolinium retention in the brain, skin, bone, liver, and other organs<sup>(23)</sup>, APTw MRI, with no contrast needed, might be a useful non-invasive technique for evaluation of brain tumor.

Moreover, APTw signal in intratumoral necrotic cystic areas showed significantly high and higher APTw value than enhancing portions. The results agreed with multiple previous studies<sup>(2,5,22,24)</sup>. This was based on the hypothesis that APT imaging detects endogenous mobile proteins and peptides in tissue such as those in the cytoplasm. The liquid-like cystic portion of the tumor shows the high APT signal, as expected, because proteinaceous cysts contain many mobile proteins. The high APT signal in the cysts could potentially lead to false positives in the clinical practice<sup>(25)</sup>. To avoid misinterpretation, combining the APT images with standard T2-weighted and FLAIR MRI, on which the cysts can readily be identified, is recommended.

The baseline APTw values of normal white matter of  $-0.4$  to  $1.4$  and cerebellum of  $1.1$  to  $1.6$  in the present study agreed with the previous study, which had white matter in the range of  $-0.03$  to  $1.64$ , and cerebellum of  $0.61$  to  $1.74$ <sup>(26)</sup>.

### Limitation

The number of cases in the present study was too small. The authors tried to increase the number of lesions by evaluating every lesion in the same patients, which might cause bias of the study.

Population bias may also have occurred because of the current results were obtained by a large number of breast cancer lesions.

### Conclusion

The present study implied that APTw MRI could be used to distinguish GBM from brain metastases by evaluating the enhancing solid portions and peritumoral non-enhancing hyperintense FLAIR areas. Both MTRAsym and nMTRAsym may be used to separate both entities. Without contrast administration, the technique could be performed repeatedly for long term follow up with no concern of gadolinium deposition in the organ, especially in the brain.

### What is already known on this topic?

Well-known advanced MRI techniques such as diffusion imaging, MR perfusion, and MR spectroscopy are used to differentiate between glioblastoma and brain metastasis. Few APTw studies have focused on differences between GBM and brain metastasis and still show discrepant results.

### What this study adds?

APTw imaging is a novel molecular non-gadolinium MRI technique used in Thailand. This study found the potential of APTw imaging to distinguish GBM from brain metastasis by both qualitative visual assessment and quantitative assessment.

### Acknowledgement

The authors gratefully acknowledge Ms. Dollaporn Polyeam for assistance with statistical analyses. The authors (DW, SP, CN, PC, OC) were funded by Chalermphakiat grant of Faculty of Medicine Siriraj Hospital.

### Conflicts of interest

The authors declare no conflict of interest.

### References

1. Zhou J, Lal B, Wilson DA, Larterra J, van Zijl PC. Amide proton transfer (APT) contrast for imaging of brain tumors. *Magn Reson Med* 2003;50:1120-6.
2. Zhou J, Zhu H, Lim M, Blair L, Quinones-Hinojosa A, Messina SA, et al. Three-dimensional amide proton transfer MR imaging of gliomas: Initial experience and comparison with gadolinium enhancement. *J Magn Reson Imaging* 2013;38:1119-28.
3. Togao O, Hiwatashi A, Yamashita K, Kikuchi K, Keupp J, Yoshimoto K, et al. Grading diffuse gliomas

- without intense contrast enhancement by amide proton transfer MR imaging: comparisons with diffusion- and perfusion-weighted imaging. *Eur Radiol* 2017;27:578-88.
4. Zhou J, Tryggstad E, Wen Z, Lal B, Zhou T, Grossman R, et al. Differentiation between glioma and radiation necrosis using molecular magnetic resonance imaging of endogenous proteins and peptides. *Nat Med* 2011;17:130-4.
  5. Ma B, Blakeley JO, Hong X, Zhang H, Jiang S, Blair L, et al. Applying amide proton transfer-weighted MRI to distinguish pseudoprogression from true progression in malignant gliomas. *J Magn Reson Imaging* 2016;44:456-62.
  6. Jiang S, Yu H, Wang X, Lu S, Li Y, Feng L, et al. Molecular MRI differentiation between primary central nervous system lymphomas and high-grade gliomas using endogenous protein-based amide proton transfer MR imaging at 3 Tesla. *Eur Radiol* 2016;26:64-71.
  7. Joo B, Han K, Choi YS, Lee SK, Ahn SS, Chang JH, et al. Amide proton transfer imaging for differentiation of benign and atypical meningiomas. *Eur Radiol* 2018;28:331-9.
  8. Yu H, Wen X, Wu P, Chen Y, Zou T, Wang X, et al. Can amide proton transfer-weighted imaging differentiate tumor grade and predict Ki-67 proliferation status of meningioma? *Eur Radiol* 2019;29:5298-306.
  9. Yu H, Lou H, Zou T, Wang X, Jiang S, Huang Z, et al. Applying protein-based amide proton transfer MR imaging to distinguish solitary brain metastases from glioblastoma. *Eur Radiol* 2017;27:4516-24.
  10. Fountas KN, Kapsalaki EZ, Gotsis SD, Kapsalakis JZ, Smisson HF 3rd, Johnston KW, et al. In vivo proton magnetic resonance spectroscopy of brain tumors. *Stereotact Funct Neurosurg* 2000;74:83-94.
  11. Krabbe K, Gideon P, Wagn P, Hansen U, Thomsen C, Madsen F. MR diffusion imaging of human intracranial tumours. *Neuroradiology* 1997;39:483-9.
  12. Chiang IC, Kuo YT, Lu CY, Yeung KW, Lin WC, Sheu FO, et al. Distinction between high-grade gliomas and solitary metastases using peritumoral 3-T magnetic resonance spectroscopy, diffusion, and perfusion imaginings. *Neuroradiology* 2004;46:619-27.
  13. Kamimura K, Nakajo M, Yoneyama T, Fukukura Y, Hirano H, Goto Y, et al. Histogram analysis of amide proton transfer-weighted imaging: comparison of glioblastoma and solitary brain metastasis in enhancing tumors and peritumoral regions. *Eur Radiol* 2019;29:4133-40.
  14. Zhou J, Payen JF, Wilson DA, Traystman RJ, van Zijl PC. Using the amide proton signals of intracellular proteins and peptides to detect pH effects in MRI. *Nat Med* 2003;9:1085-90.
  15. Togao O, Yoshiura T, Keupp J, Hiwatashi A, Yamashita K, Kikuchi K, et al. Amide proton transfer imaging of adult diffuse gliomas: correlation with histopathological grades. *Neuro Oncol* 2014;16:441-8.
  16. Law M, Cha S, Knopp EA, Johnson G, Arnett J, Litt AW. High-grade gliomas and solitary metastases: differentiation by using perfusion and proton spectroscopic MR imaging. *Radiology* 2002;222:715-21.
  17. Kogan F, Hariharan H, Reddy R. Chemical Exchange Saturation Transfer (CEST) imaging: Description of technique and potential clinical applications. *Curr Radiol Rep* 2013;1:102-14.
  18. Lu J, Cai C, Cai S, Chen Z, Zhou J. Chemical exchange saturation transfer MRI using intermolecular double-quantum coherences with multiple refocusing pulses. *Magn Reson Imaging* 2014;32:759-65.
  19. Bai Y, Lin Y, Zhang W, Kong L, Wang L, Zuo P, et al. Noninvasive amide proton transfer magnetic resonance imaging in evaluating the grading and cellularity of gliomas. *Oncotarget* 2017;8:5834-42.
  20. Zamecnik J. The extracellular space and matrix of gliomas. *Acta Neuropathol* 2005;110:435-42.
  21. Park JE, Kim HS, Park KJ, Kim SJ, Kim JH, Smith SA. Pre- and posttreatment glioma: Comparison of amide proton transfer imaging with MR spectroscopy for biomarkers of tumor proliferation. *Radiology* 2016;278:514-23.
  22. Suh CH, Park JE, Jung SC, Choi CG, Kim SJ, Kim HS. Amide proton transfer-weighted MRI in distinguishing high- and low-grade gliomas: a systematic review and meta-analysis. *Neuroradiology* 2019;61:525-34.
  23. Ramalho J, Semelka RC, Ramalho M, Nunes RH, AlObaidy M, Castillo M. Gadolinium-based contrast agent accumulation and toxicity: An update. *AJNR Am J Neuroradiol* 2016;37:1192-8.
  24. Zhou J, Heo HY, Knutsson L, van Zijl PCM, Jiang S. APT-weighted MRI: Techniques, current neuro applications, and challenging issues. *J Magn Reson Imaging* 2019;50:347-64.
  25. Lu J, Zhou J, Cai C, Cai S, Chen Z. Observation of true and pseudo NOE signals using CEST-MRI and CEST-MRS sequences with and without lipid suppression. *Magn Reson Med* 2015;73:1615-22.
  26. Sartoretti T, Sartoretti E, Wyss M, Schwenk Á, Najafi A, Binkert C, et al. Amide proton transfer contrast distribution in different brain regions in young healthy subjects. *Front Neurosci* 2019;13:520.